# Manifestation of Kohn Anomaly in $1/f$ Fluctuations in Metallic Carbon Nanotubes

Ju Hee Back,[1] Cheng-Lin Tsai,[1] Sunkook Kim,[2] Saeed Mohammadi,[2] and Moonsub Shim[1,*]

[1]*Department of Materials Science and Engineering, University of Illinois, Urbana, Illinois 61801, USA*
[2]*School of Electrical and Computer Engineering and Birck Nanotechnology Center, Purdue University, West Lafayette, Indiana 47907, USA*

(Received 20 April 2009; published 16 November 2009)

Low-frequency noise in metallic single walled carbon nanotubes is shown to be strongly dependent on the Fermi level position and the applied electric field across the nanotube. Resonance-like enhancement observed near optical phonon energy only when the Fermi level lies near the Dirac point is correlated to Raman *G*-band softening and broadening. The results suggest that the competition between zone-center and zone-boundary phonon scattering is the underlying origin of the large enhancement and resonance-like behavior of $1/f$ noise.

DOI: 10.1103/PhysRevLett.103.215501 PACS numbers: 63.20.kd, 63.22.Gh, 73.63.Fg, 78.67.Ch

In addition to facilitating studies in correlated electrons [1], Kohn anomalies [2], and novel chemistries [3], metallic carbon nanotubes (CNTs) may serve as next-generation transparent conductors and high-speed interconnects. For such applications that require relatively high fields, electron-optical phonon interactions become important. Optical phonon scattering is known to govern ballistic transport, current saturation, and negative differential conductance behaviors [4–8]. However, no studies to date have dealt with current *fluctuations* arising from optical phonon scattering in CNTs. Such fluctuations may define how high current carrying capacity [4] and ballistic transport characteristics [5,6] may be exploited. Optical phonon contributions to the predominant fluctuation, the $1/f$ noise, is then of particular importance. Field and Fermi level ($E_F$) position dependent $1/f$ noise in metallic CNTs presented here demonstrates such contributions.

Single walled CNTs were grown by chemical vapor deposition utilizing patterned $Fe(NO_3)_3 \cdot 9H_2O$ and alumina or ferritin (Sigma) catalysts with $CH_4$ and $H_2$. For electrical contacts, Au (35 nm with 5 nm Ti wetting layer) electrodes with 4 $\mu$m channel lengths were patterned on top of CNTs grown on Si substrates with 350 nm thermal oxide. Polymer electrolyte consisting of 4:1 weight ratio of polyethylenimine (Aldrich, low molecular weight) and $LiClO_4 \cdot 3H_2O$ was spin coated on top of electrically contacted CNTs and electrochemical gate potential was applied with a nearby electrode [9]. Low-frequency current noise spectra were obtained with a current amplifier (Stanford Research Systems SR 570 or a home-built system) and a dynamic signal analyzer (HP 35670A or HP 35665A). Unless otherwise noted, the values of noise amplitude $A$ were obtained from the measured noise spectra $S_I$ and the drain-source current $I_{ds}$ over the entire frequency ($f$) range studied here using the relation $S_I/I_{ds}^2 = A/f$. As shown in Ref. [10], the polymer electrolyte does not introduce additional noise. Raman measurements were carried out on a Jobin Yvon LabRam HR 800 micro-Raman spectrometer with a 633 nm (1.96 eV) excitation source and a 100× air objective. All measurements were carried out at room temperature under ambient conditions.

In the scale down of devices, the possibility of increasing $1/f$ noise has been of significant concern. Interestingly, several reports have now shown that the magnitude of these low-frequency fluctuations in individual CNT-based devices is comparable to those of bulk semiconductor devices [10–16]. Recent studies have even revealed that careful fabrication approaches can reduce the noise amplitude [17] with the lowest $1/f$ noise amplitude ($A$) of $\sim 10^{-5}$ being reported in individual metallic CNTs where the underlying substrate has been etched away [18]. Figure 1 shows that an order of magnitude smaller $A$, as low as $\sim 1.5 \times 10^{-6}$ at a low bias across the CNT ($V_{ds}$) of 50 mV, can be achieved even if the metallic CNT is resting on the substrate. Here,

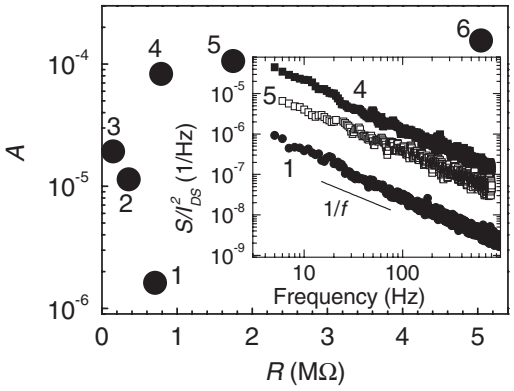


FIG. 1. Noise amplitude $A$ in metallic CNT devices. Comparison of $A$ of 6 different devices with their corresponding resistance ($R$) is shown in the main panel. Devices are labeled 1–6 for convenience and as referred to in the subsequent figures. Noise spectra $S_I$ normalized to the square of the drain-source current $I_{ds}^2$ for three different metallic CNT devices are shown in the inset. Numbers 1, 4, and 5 indicate the corresponding devices labeled in the main panel.

 

we refer to low bias regime when $eV_{ds} < \hbar\omega_q$ where $e$ is the electric charge, $\hbar$ is the Planck's constant, and $\omega_q$ is the optical phonon frequency with $q$ corresponding to either $\Gamma$-point optical phonon ($q = \Gamma$) or the $K$- or $K'$-point zone-boundary phonon ($q = K$). $\Gamma$- and $K$-point phonons are the two optical phonons that are important in carrier scattering in the high-field limit [5]. Examples of frequency dependence of $S_I$ for three different metallic CNTs are shown in the inset of Fig. 1.

The large range of $A$ values obtained for the on-substrate metallic CNTs in Fig. 1 may not be too surprising given the possible large variations in the local chemical environment [19] and given similar large range of $A$ observed in semiconducting CNTs [10]. Extrinsic factors such as the substrate and contacts can significantly influence the observed $1/f$ noise. However, all 6 metallic CNTs studied here exhibit varying degree of enhancement in $S_I$ and therefore in $A$ at $eV_{ds}$ slightly above $\hbar\omega_\Gamma$ (0.196 eV) only when $E_F$ is near the Dirac point (DP). They also exhibit linear $I_{ds}$-$V_{ds}$ characteristics in the voltage range studied as exemplified in the inset of Fig. 2(a). When $A$ is small ($\sim 10^{-4}$ or less) in the low $V_{ds}$ limit, this enhancement is easily observed. As seen in Fig. 2(b), when $V_g = 0$ V, $S_I$ at a fixed frequency increases linearly with the square of $I_{ds}$ as expected from the relation $S_I/I_{ds}^2 = A/f$. At the same $V_g$, the noise amplitude $A$ remains essentially independent of $V_{ds}$. However, at $V_g = -1.2$ V, a sharp rise in both $S_I$ and $A$ near $V_{ds} \sim -0.2$ V is observed. Such an enhancement in $A$ is also observed in the positive $V_{ds}$ regime as shown in Fig. 2(d). The $V_g$ dependence of $I_{ds}$ in Fig. 2(a) shows that the current minimum is near $V_g \sim -1.2$ V whereas $V_g = 0$ V corresponds to the current maximum. That is, the resonance-like enhancement of $S_I$ and $A$ for $eV_{ds} \sim \hbar\omega_\Gamma$ occurs only at $V_g$ corresponding to $E_F$ being near DP. Similar enhancement of $A$ at $eV_{ds} \sim \hbar\omega_\Gamma$ and $E_F \sim$ DP for another metallic CNT is shown in Fig. 3(a).

In Fig. 3(b), we also plot the values of $A$ obtained from taking into account slight variations in the $1/f$ dependence of $S_I$, that is, when we allow $\gamma$ in $1/f^\gamma$ to vary as a fitting parameter rather than fixing $\gamma = 1$. Typically, $\gamma$ is very close to 1, but it does sometimes vary as much as from 0.8 to 1.2 (most values are $1 \pm 0.1$). These deviations in $\gamma$ may potentially affect the actual value of $A$. However, a comparison of Figs. 3(a) and 3(b) shows that, while the baseline values—i.e., at the very low and very high $V_{ds}$ regimes—can be different, the enhancement effect at $eV_{ds} \sim \hbar\omega_\Gamma$ remains the same. These variations in $\gamma$ are likely originating from a distribution of carrier traps [10,20], either from the substrate or the contacts but do not alter the resonance-

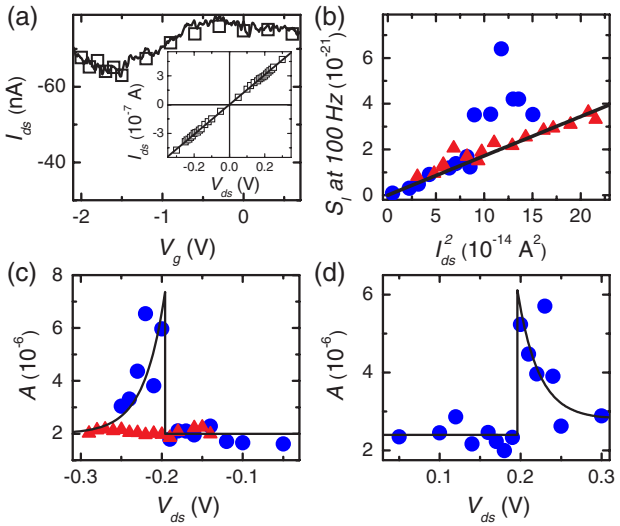


FIG. 2 (color online). (a) Gate voltage $V_g$ and the drain-source voltage $V_{ds}$ (inset) dependences of current $I_{ds}$ of a metallic CNT (labeled as device "1" in Fig. 1). Solid line and open squares represent data collected before and during $1/f$ noise measurements, respectively. Solid line in the inset is a linear fit. The gate dependence of $I_{ds}$ can be observed even in a metallic CNT due to the high efficiency of polymer electrolyte gating. (b) $I_{ds}{}^2$ dependence of the noise spectrum $S_I$ at 100 Hz at two different gate voltages ($V_g$). Line is linear fit for the red triangles. (c) $V_{ds}$ dependence of noise amplitude $A$ at two different $V_g$. (d) Same as (c) for one $V_g$ near Dirac point and positive $V_{ds}$. Lines in (c) and (d) show exponential decay for $e|V_{ds}| > \hbar\omega_\Gamma$. For data in (b)–(d), blue circles correspond to $V_g = -1.2$ V (near the Dirac point) and red triangles correspond to $V_g = 0$ V (away from Dirac point).

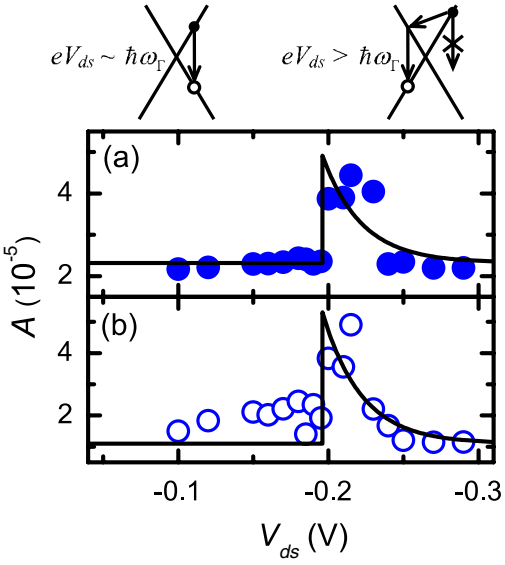


FIG. 3 (color online). $V_{ds}$ dependence of $A$ of a metallic CNT device labeled as "3" in Fig. 1 when the Fermi level is near the Dirac point ($V_g = -0.1$ V). Filled circles (a) are values of $A$ obtained with fixed exponent $\gamma = 1$ in $1/f^\gamma$ dependence of $S_I$ whereas the open circles (b) are values obtained with $\gamma$ allowed to vary. Lines show exponential decay for $e|V_{ds}| > \hbar\omega_\Gamma$ in both cases. The schematic on top is a representation of $\Gamma$-point optical phonon scattering near the Dirac point when $eV_{ds}$ is equal to the optical phonon energy $\hbar\omega_\Gamma$ and when it is sufficiently larger than $\hbar\omega_\Gamma$.

like enhancement in $A$. Furthermore, as exemplified in Fig. 2(b), the enhancement is also present in $S_I$ which does not suffer from potential problems associated with the variations in $\gamma$. Hence, processes involving optical phonons, rather than the slight variations in $\gamma$, are the origin of the observed $1/f$ noise enhancement.

The enhancements of $S_I$ and $A$ resonant with $\mathbf{\Gamma}$-point phonon energy are rather surprising in that the zone-boundary $K$-point phonons with faster scattering rates are expected to dominate the high-field transport characteristics in metallic CNTs [5–7]. That is, one might expect a rise in the noise amplitude near the onset of $K$ phonon scattering ($\hbar\omega_K = 0.161$ eV) without the resonance-like behavior. It is even more unusual that this enhancement occurs only at a particular $E_F$ position. To explain these results, we consider the $\mathbf{\Gamma}$ and $K$ phonon scattering rates and how they may vary with $V_{\rm ds}$ and $E_F$. Here, we consider only phonon emission. Following Refs. [21,22], we include $E_F$ and diameter ($d$) dependences in the scattering rate as

$$\frac{1}{\tau_q} = \frac{a_o^2\sqrt{3}}{2\pi d M \nu_F \hbar\omega_q}\langle D_q^2\rangle\left[\frac{1}{e^{(E_F-\hbar\omega_q/2)/k_BT}+1} - \frac{1}{e^{(E_F+\hbar\omega_q/2)/k_BT}+1}\right], \quad (1)$$

where $a_o$ is the graphene lattice spacing, $M$ is the atomic mass, $\nu_F$ is the Fermi velocity, $\langle D_q^2\rangle$ is the graphene electron-phonon coupling, $k_B$ is the Boltzman constant, and $T$ is the temperature. Following Ref. [8], if we use $a_o = 2.46$ Å, $\nu_F = 8.4\times10^5$ m/s, $\langle D_K^2\rangle = 92.05$ (eV/Å)$^2$ and $\langle D_\Gamma^2\rangle = 45.6$ (eV/Å)$^2$, $\tau_K \approx 1.1\times10^{-13}$ s and $\tau_\Gamma \approx 2.7\times10^{-13}$ s for a 1 nm diameter metallic CNT when $E_F$ is near DP (defined as $E_F = 0$ eV). While the reported values of $\langle D_q^2\rangle$ vary significantly [2,5,23], as discussed later, it is the ratio of $\langle D_\Gamma^2\rangle/\langle D_K^2\rangle$ that is important here, not the absolute values. This ratio is similar across different reports leading to $\tau_\Gamma/\tau_K$ ranging from ~2 to 5. For $\hbar\omega_K \le eV_{\rm ds} < \hbar\omega_\Gamma$, the fraction of electrons scattered by emitting a zone-boundary phonon is $N_K/N = (1 - e^{-t/\tau_K})$. Given the CNT length $l_{NT}$ of 4 $\mu$m, the lower limit of average total time $t_{\rm total}$ that an electron spends in the CNT is $\sim5\times10^{-12}$ s (assuming velocity $\nu_F$). Then, the average time $t$ that an electron spends in the CNT *after* accelerating and attaining enough energy to emit a zone-boundary phonon is $t = t_{\rm total} - \hbar\omega_K l_{NT}/(\nu_F e V_{\rm ds})$. Since $t$ is already about 3 times larger than $\tau_K$ at $V_{\rm ds} = 0.171$ V (10 meV above $\hbar\omega_K$) even in the lower limit of $t_{\rm total}$, essentially all electrons are scattered by the zone-boundary phonons for $eV_{\rm ds}$ a few meV above $\hbar\omega_K$ (e.g., $N_K/N = 0.92$ for $V_{\rm ds} = 0.171$ V). While there may be a slight increase in $A$ near the $K$-point phonon energy especially in Figs. 2(c) and 3(b), the change is small indicating that whether all or no electrons are scattered by zone-boundary phonons, the resulting $1/f$ noise behavior is similar. Since all electrons are likely to be scattered by the same phonon, all carriers behave similarly and therefore do not deviate much from the average behavior—i.e., small fluctuations.

For $eV_{\rm ds} \ge \hbar\omega_\Gamma$, we now have to consider scattering by both $\mathbf{\Gamma}$ and $K$-point phonons. Noting again that $t \gg \tau_K$, the ratio of $K$-point to $\mathbf{\Gamma}$-point phonon scattered electrons $N_K/N_\Gamma$ is equal to $\tau_\Gamma/\tau_K$ or 2.5 using $\langle D_q^2\rangle$ values given above. Rather than one process dominating, now there are two competing scattering processes. Since these two processes are likely to result in different behaviors (i.e., either different mobility change or carrier number change), electrons may be expected to behave significantly differently from the average behavior—i.e., large fluctuations. However, as $eV_{\rm ds}$ becomes larger than about $k_BT$ above $\hbar\omega_\Gamma$, $\mathbf{\Gamma}$ phonon emission will not occur unless there is an additional acoustic phonon scattering as schematically shown in Fig. 3. Then, zone-boundary phonon scattering again dominates in this regime leading to $A$ similar to $eV_{\rm ds} < \hbar\omega_\Gamma$ region. Noting that a similar situation occurs when the applied $V_g$ shifts $E_F$ away from DP for fixed $eV_{\rm ds} \sim \hbar\omega_\Gamma$, then the optical phonon scattering contribution to $A$ for $eV_{\rm ds} \ge \hbar\omega_\Gamma$ may be expressed as being proportional to $\exp\{-[(e|V_{\rm ds}| + |E_F|) - \hbar\omega_\Gamma]/k_BT\}$. Here, the absolute values reflect the symmetry between electrons and holes. The lines in Figs. 2(c), 2(d), 3, and 4(b) inset are curve fits using this exponential dependence with a preexponential and a constant offset as the only fitting parameters.

To further verify that the unusual enhancement of $1/f$ noise occurring only when $eV_{\rm ds} \sim \hbar\omega_\Gamma$ and $E_F$ near DP is associated with $\mathbf{\Gamma}$ phonon scattering, we correlate above results to $E_F$ dependent Raman $G$-band linewidth [24]. It is now well-established that conduction electron excitations couple to $\mathbf{\Gamma}$ LO phonon transitions leading to the observed softening and broadening of the lower frequency $G$-band mode in the Raman spectrum [21,22,25–28]. This electron-phonon coupling is particularly strong near DP where the bands cross leading to a logarithmic divergence of the phonon frequency known as the Kohn anomaly [2,25]. Figure 4(a) shows Raman $G$-band spectra of a metallic CNT at the indicated $V_g$. As expected, broadening and softening of the $\mathbf{\Gamma}$ LO mode due to the Kohn anomaly is observed at $E_F$ near DP ($V_g \sim 0.6$ V). The inset of Fig. 4(b) shows that the resonance-like behavior can again be observed near $eV_{\rm ds} \sim \hbar\omega_\Gamma$ at $E_F$ near DP. In the main panel of Fig. 4(b), we compare $V_g$ dependences of $A$ and the $\mathbf{\Gamma}$ LO mode linewidth (FWHM$_\Gamma$) of this CNT. Both show maximum value near DP. Since FWHM$_\Gamma \propto 1/\tau_\Gamma$, the $V_g$ (or $E_F$) dependence arises from the Fermi-Dirac distribution terms in Eq. (1), the fitting result of which is shown by the dashed line. On the other hand, the main $V_g$ dependence of $A$ comes from the direct exponential decay about DP as described earlier which is used to fit the data [29]. Hence, we expect a sharper decrease in $A$ than in FWHM$_\Gamma$ as $E_F$ shifts away from DP and indeed observe

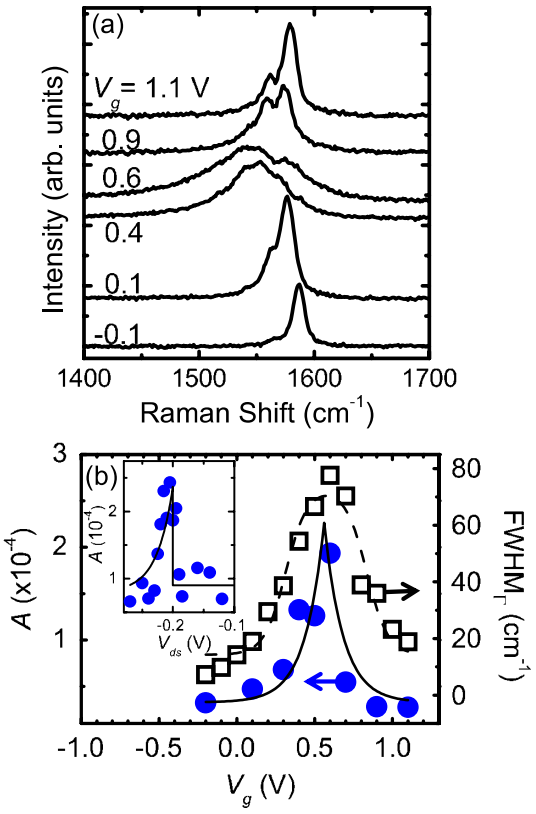


FIG. 4 (color online). Correlation between Raman $G$-band phonon softening or broadening with resonance-like enhancement of noise amplitude $A$ near the Dirac point for the metallic nanotube device labeled as "4" in Fig. 1. $G$-band region of the Raman spectrum at the indicated gate voltages ($V_g$) is shown in (a). Comparison of $V_g$ dependence of full width at half maximum of $G$-band LO mode (FWHM$_\Gamma$) with that of $A$ is shown in (b). $V_g$ dependence of $A$ is collected at $V_{ds} = -0.2$ V. Lines are curve-fitting results as described in the text. The inset shows the $V_{ds}$ dependence of $A$ near the Dirac point.

this behavior in Fig. 4(b). This correlation between LO phonon linewidth (and therefore the scattering rate) and $A$ indicates the importance of optical phonon scattering in $1/f$ noise of metallic CNTs.

Although imperfections at surfaces, interfaces, and contacts have often been the focus of low-frequency noise in nanoscale devices, our results demonstrate that intrinsic properties such as the strong electron-phonon coupling can profoundly affect noise characteristics. The fact that all six metallic CNT devices exhibit similar enhancement around LO phonon resonance near DP despite their differences in the local variations in the substrate and contacts is an indication that the noise enhancement observed here is not likely to be correlated to extrinsic factors. While further work is necessary to ascertain whether the mechanism involves carrier mobility or number fluctuations, $V_{ds}$ and $E_F$ dependences and the correlation to the Raman $G$-band broadening presented here reveal that the underlying origin of the resonance-like enhancement in the $1/f$ noise is the optical phonon scattering. With faster rates, zone-boundary phonon scattering is expected to be the most dominant factor in determining high-field electron transport characteristics in metallic CNTs. In contrast, we have shown here that $\Gamma$-point LO phonon scattering, when it competes with $K$-point phonon, dictates $1/f$ fluctuations. Interestingly, LO phonon scattering contributions to $1/f$ noise can be suppressed at fields sufficiently above the phonon resonance or simply by ensuring that $E_F$ lies away from DP. These results reveal manifestations of Kohn anomaly in the observed $1/f$ noise behavior. With optical phonon contributions easily separated out even at room temperature, our results also suggest that metallic CNTs might serve as an excellent experimental platform to shed light on intrinsic vs extrinsic origins of $1/f$ noise in nanoscale devices.

This material is based upon work supported by the NSF (Grants No. CCF-0506660 and No. DMR-0348585).

*mshim@illinois.edu

[1] V. V. Deshpande *et al.*, Science **323**, 106 (2009).
[2] S. Piscanec *et al.*, Phys. Rev. Lett. **93**, 185503 (2004).
[3] K. Kamaras *et al.*, Science **301**, 1501 (2003).
[4] Z. Yao, C. L. Kane, and C. Dekker, Phys. Rev. Lett. **84**, 2941 (2000).
[5] J.-Y. Park *et al.*, Nano Lett. **4**, 517 (2004).
[6] A. Javey *et al.*, Phys. Rev. Lett. **92**, 106804 (2004).
[7] E. Pop *et al.*, Phys. Rev. Lett. **95**, 155505 (2005).
[8] M. Lazzeri *et al.*, Phys. Rev. Lett. **95**, 236802 (2005).
[9] G. P. Siddons *et al.*, Nano Lett. **4**, 927 (2004).
[10] J. H. Back *et al.*, Nano Lett. **8**, 1090 (2008).
[11] Y.-M. Lin *et al.*, Nano Lett. **6**, 930 (2006).
[12] M. Ishigami *et al.*, Appl. Phys. Lett. **88**, 203116 (2006).
[13] F. Liu *et al.*, Appl. Phys. Lett. **89**, 063116 (2006).
[14] J. Appenzeller *et al.*, IEEE Trans. Nanotechnol. **6**, 368 (2007).
[15] D. Tobias *et al.*, Phys. Rev. B **77**, 033407 (2008).
[16] J. Mannik *et al.*, Nano Lett. **8**, 685 (2008).
[17] S. K. Kim *et al.*, Appl. Phys. Lett. **90**, 163108 (2007).
[18] Y.-M. Lin *et al.*, Nanotechnology **18**, 295202 (2007).
[19] M. Shim *et al.*, J. Phys. Chem. C **112**, 13017 (2008).
[20] J. I. Lee, J. Brini, A. Chovet, and C. A. Dimitriadis, Solid-State Electron. **43**, 2181 (1999).
[21] M. Lazzeri *et al.*, Phys. Rev. B **73**, 155426 (2006).
[22] N. Caudal *et al.*, Phys. Rev. B **75**, 115423 (2007).
[23] G. D. Mahan, Phys. Rev. B **68**, 125409 (2003).
[24] K. T. Nguyen, A. Gaur, and M. Shim, Phys. Rev. Lett. **98**, 145504 (2007).
[25] K. Ishikawa and T. Ando, J. Phys. Soc. Jpn. **75**, 084713 (2006).
[26] Y. Wu *et al.*, Phys. Rev. Lett. **99**, 027402 (2007).
[27] H. Farhat *et al.*, Phys. Rev. Lett. **99**, 145506 (2007).
[28] A. W. Bushmaker *et al.*, Nano Lett. **9**, 607 (2009).
[29] Here, we introduce one additional parameter to take into account the nonideal gate efficiency for both FWHM$_\Gamma$ and $A$.